

# Thermal properties and flammability of nanocomposites based on diene rubbers and naturally occurring and activated halloysite nanotubes

Przemysław Rybiński · Grażyna Janowska ·  
Małgorzata Józwiak · Agnieszka Pająk

Received: 16 March 2011 / Accepted: 1 July 2011 / Published online: 19 July 2011  
© The Author(s) 2011. This article is published with open access at Springerlink.com

**Abstract** This article presents a procedure of the activation of halloysite and a method of the synthesis of nucleus-sheath type filler. The effects of the nanoadditives obtained on the thermal properties, flammabilities and fire hazards of peroxide and sulfur vulcanizates of NBR and SBR rubbers, are discussed. Based on the test results obtained by derivatography, oxygen index, FAA micro-calorimeter and cone calorimeter, the thermal stability, flammability, and fire hazard of the nanocomposites investigated were determined. The results obtained were interpreted from the point of view of the chemical structure of the diene elastomers investigated, their spatial network structure, and the method of halloysite modification.

**Keywords** Halloysite · Thermal stability · Vulcanizate of diene rubbers · Flammability · Fire hazard

## Introduction

Along with the development of nanotechnology, ever-increasing interest has been focused on nanofillers, such as nanosilica, zinc nanooxide, or natural aluminosilicates, which are now successfully used in both elastomeric composites and thermoplastics.

Polymeric composites containing appropriately modified nanofillers show considerably better functional properties compared with traditional materials. Even a low quantity of a nanoadditive (1–8 phr) incorporated into a polymeric matrix allows one to obtain materials with specific properties, i.e., resistant to the action of considerably lowered or elevated temperatures, showing good mechanical properties, as well as reduced flammability and fire hazard. Both the reduced flammability and fire hazard are of paramount importance from the point of view of health and life protection as well as for economic reasons.

In recent years, polymeric nanocomposites containing modified montmorillonites have been a subject of many research and implementation studies [1–3]. So far, however, not much attention has been devoted to naturally occurring aluminosilicate nanotubes. Their use in elastomeric matrix remains largely unexamined.

Halloysite ( $\text{Al}_2[\text{Si}_2\text{O}_5(\text{OH})_4]\cdot 2\text{H}_2\text{O}$ ) is a mineral combining the chemism and rigidity of montmorillonite with the geometry of carbon nanotubes [4, 5]. A halloysite nanotube (HNT) occurs in the form of two-layer aluminosilicate. Two tetrahedral silica layers are octahedrally connected with aluminum atoms, resulting in a cylindrical shape of HNT particles [6, 7]. From a mineralogical point of view, halloysite is a mineral, similar to kaolin and is a weathering product of granitic and rhyolitic volcanic rocks [8]. The length of HNTs varies from 1 to 15  $\mu\text{m}$  and their diameter from 10 to 150 nm. Therefore, halloysite is characterized by a high coefficient of shape (L/D ratio) [4–7], and consequently, when incorporated into a polymeric matrix, it shows a considerably larger surface of polymer–filler interaction in relation to conventional fillers. Hence, it reduces the oscillation of polymer chain segments, bringing about an increase in degradation and destruction temperatures of polymers filled with halloysite.

---

P. Rybiński (✉) · M. Józwiak  
Department of Management and Protection Environment,  
Jan Kochanowski University of Humanities and Sciences  
in Kielce, Kielce, Poland  
e-mail: przemek100@ujk.kielce.pl

G. Janowska · A. Pająk  
Institute of Polymer and Dye Technology,  
Technical University of Łódź, Lodz, Poland

This article presents the results of assessing the effect of halloysite activated with sulfuric acid on the thermal stability and flammability of crosslinked diene rubbers. An intercalated halloysite was also used to prepare a filler of nucleus-sheath type.

## Experimental

### Materials

We examined the following diene rubbers: butadiene–styrene rubber, KER 1500, containing 23.5% of combined styrene, from Synthos S.A, and butadiene–acrylonitrile rubber, NBR 2255V, containing 22% of combined acrylonitrile from Bayer.

The rubbers were crosslinked by means of dicumyl peroxide (DCP) in the presence of zinc oxide (ZnO), or with the use of sulfur in the presence of ZnO and *N*-cyclohexyl-2-benzoyl sulfenamide (Tioheksam CBS). The peroxide vulcanizates of butadiene–styrene and butadiene–acrylonitrile rubbers were denoted with SN and NN symbols, respectively. The sulfur vulcanizates of butadiene–styrene and butadiene–acrylonitrile rubbers were denoted with SS and NS symbols, respectively.

Halloysite derived from Dunino deposit, near Legnica (Poland), was used as a filler of elastomeric blends. The chemical composition of this aluminosilicate, before and after its acidic activation, was determined by means of a micro-analyzer, type EDS EDAX Genesis XM 4i (USA), used in a Quanta 250 FEG electron microscope. The activation of halloysite with a 30% H<sub>2</sub>SO<sub>4</sub> for 20 min was performed to expose HNTs by removing higher aluminosilicate acids (so-called allophane acids) from their surface and space between them as shown in Fig. 1.

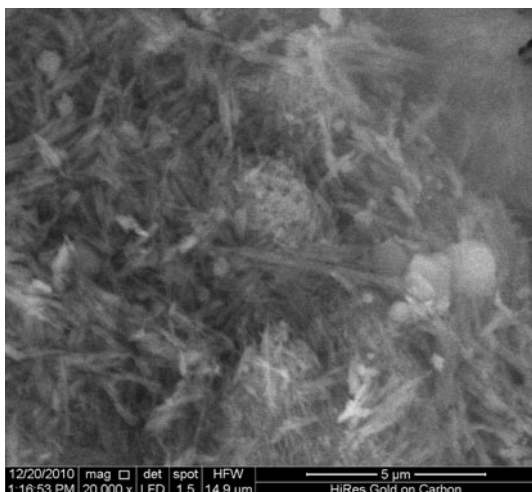


**Fig. 1** Halloysite from Aldrich

The nucleus-sheath type filler of a new generation was prepared by the plasticization of acid-intercalated halloysite with chlorosulfonated polyethylene (CSM), Hypalon 30, containing 43% of combined chlorine, provided by DuPont Dow Elastomers. The resultant premix masterbatch was then heated in a Nabertherm muffle furnace under a neutral gas up to 350 °C. The chlorine content in this filler was 7.53% by wt. [9].

### Methods

Non-intercalated and intercalated halloysites were assessed by means of a Quanta 250 FEG electron microscope (FEI Company) equipped with electron gun and field emission (Schottky's emitter).

Elastomeric blends were prepared at room temperature by means of a laboratory roll mill, followed by vulcanization in steal molds placed between electrically heated press plates. The optimal time of vulcanization ( $\tau$  0.9) at a temperature of 160 °C was determined by means of a WG-2 vulcameter according to Standard PN-ISO 3417:1994.

The thermal properties of halloysite and halloysite-containing vulcanizates were tested under air atmosphere within the temperature range of 25–800 °C, by means of a Paulik, Paulik, Erdey derivatograph, using Al<sub>2</sub>O<sub>3</sub> as a reference substance. The heating rate for a sample of weight 90 mg was 7.9 °C/min, and the sensitivities of thermal curves were as follows:  $TG = 100$ ,  $DTA = 1/5$ , and  $DTG = 1/30$ .

The flammability of vulcanizates was determined by the method of oxygen index (OI) using an apparatus from Fire Testing Technology Limited. For flammability tests, 50 × 10 × 4 mm samples were prepared. Using a constant nitrogen flow rate amounting to  $40 \pm 2 \text{ mm} \times \text{s}^{-1}$ , through a test column with a diameter of 75 mm, the oxygen concentration was selected so that the sample under testing was burned within time,  $t = 180 \text{ s}$ . The sample top was ignited for 5 s by means of a propane–butane gas burner. The numerical value of OI was calculated from the following formula:

$$OI = (C_F + k \times d) \div 100$$

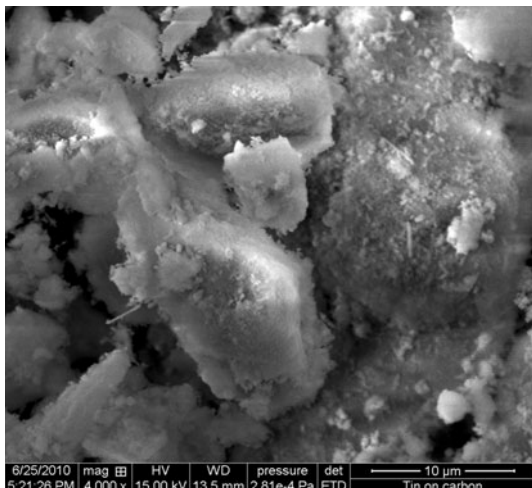
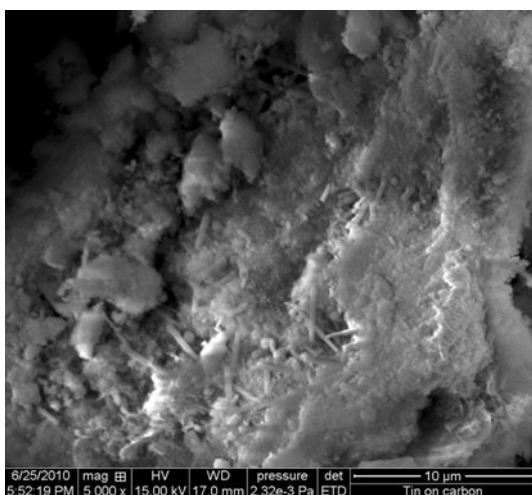
where  $C_F$  is the final oxygen concentration, at which a sample is burned within 180 s;  $d$  is the step size between oxygen concentration changes during the test procedure;  $k$  is the coefficient of proportionality.

We also tested flammability in air using identical samples as in the case of OI method. A sample in a vertical position was ignited with a gaseous burner as before for 5 s, and its combustion time ( $T_s$ ) was measured.

The vulcanizates under investigation were examined by means of an FAA micro-calorimeter from Fire Testing Technology Limited. The temperature of pyrolyzer was 750 °C, while that of combustor was 900 °C. During measurement, the following parameters were recorded: ignition

**Table 1** Results of elementary analysis of halloysite

Sample	C/%	Al/%	Si/%	Fe/%	O/%	S/%
Halloyiste	46	9	8	3	34	–
Activated halloysite	24	6.7	25.3	1.9	41	1.1

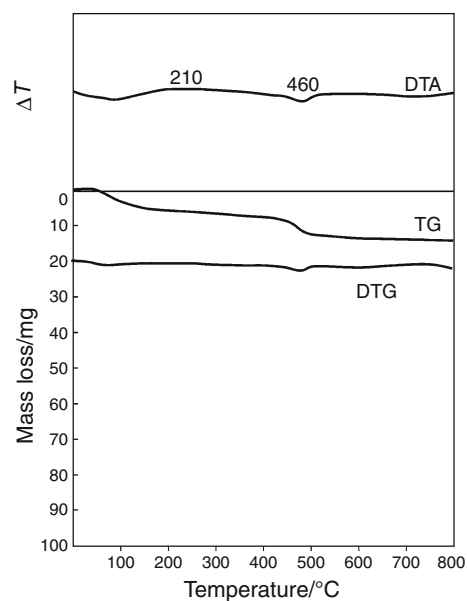
**Fig. 2** Non-activated halloysite**Fig. 3** Activated halloysite

temperature, maximal heat emission rate, total heat emitted, heat capacity, and percentage oxygen consumption.

Selected samples were tested using a cone calorimeter from Atlas Electric Devices Company.

## Results and discussion

The activation of halloysite with a 30%  $\text{H}_2\text{SO}_4$  for 20 min was performed to expose HNTs by removing higher

**Fig. 4** TG, DTG, and DTA curves of activated halloysite

aluminosilicate acids from their surfaces and spaces between them as shown in Fig. 1.

Based on the results obtained using EDS micro-analyzer, it was found that the intercalation of halloysite performed in this study changed its elementary composition (Table 1).

The unmodified halloysite contains considerable amounts of carbon and iron (Table 1). Carbon in the form of carbonates and overall organic carbon is on the surface of aluminosilicate; therefore, the surface-performed elementary analysis of non-activated halloysite indicates only 8% silicon content in it. The intercalation of halloysite with sulfuric acid removes considerable amounts of carbon and iron salts from its surface, which exposes the tubular structure of halloysite as indicated by both the considerable increase in silicon content by about 320% compared to non-activated halloysite (Table 1) and the electron microscopy photos (Figs. 2, 3).

During activation with acid, besides the overall organic carbon, a considerable portion of aluminosilicate acids is washed out, which decreases the percentage contents of aluminum and silicon in the activated halloysite sample analyzed. It is not unlikely that some nanotubes are destroyed during the acidic intercalation.

From the derivatographic analysis of activated halloysite, it follows that it undergoes clear three-stage decomposition within the temperature range of 30–700 °C (Fig. 4). Its first stage of thermal decomposition taking place at  $\Delta T_1 = 30\text{--}100$  °C, accompanied by the endothermic process recorded in DTA curve, is due to desorption of water (5.5%) combined with the aluminosilicate surface. The second stage of thermal decomposition

proceeds at  $\Delta T_2 = 100\text{--}420\text{ }^\circ\text{C}$ , being connected with the release of water physically occluded in nanotubes, as well as water chemically combined with the halloysite surface. This stage is accompanied by a sample weight loss of 3.4%. The final stage of thermal decomposition at  $\Delta T_3 = 420\text{--}700\text{ }^\circ\text{C}$  is connected with the combustion of the carbon fraction occurring in the form of carbonates and overall aromatic carbon. This stage is accompanied by a sample weight loss of about 6% [4, 10].

The results of thermal examinations show that the characteristics of DTA, TG, and DTG curves of crosslinked elastomers, such as butadiene–acrylonitrile (NBR) or butadiene–styrene copolymer (SBR), are not significantly affected by the spatial network structure and the content of nanoadditive (Fig. 5). On the other hand, the thermal stabilities of elastomers depends on the method of crosslinking, and hence on the spatial network structure [11, 17]. The use of sulfur as a crosslinker leads to the formation of crosswise sulfide bonds that are considerably weaker than the carbon–carbon bonds resulting from the crosslinking by means of dicumyl peroxide. The thermal stabilities of the peroxide vulcanizate of nitrile rubber (NN) and the peroxide vulcanizate of SBR rubbers (SN) determined with coefficient  $T_5$ , are higher by  $50\text{ }^\circ\text{C}$  than those of sulfur vulcanizates denoted with NS (sulfur vulcanizate of NBR rubber) and SS (sulfur vulcanizate of SBR rubber), but when expressed by  $T_{50}$ , they are higher by about  $20\text{ }^\circ\text{C}$  (Table 2).

The results of derivatographic analysis listed in Table 2 show that activated halloysite does not unmistakably

influence the thermal stabilities of the vulcanizates investigated. In most of the cases, the aluminosilicate used does not significantly change the thermal stabilities of the vulcanizates determined with coefficients  $T_5$  and  $T_{50}$ .

It is the thermal decomposition rate that is an important parameter determining both the thermal stability of a polymeric material and its flammability. The decrease in the destruction rate of polymeric nanocomposites exerts a positive influence on the reduction in their flammability. This is due to the formation of lower amounts of volatile and flammable products of pyrolysis passing to flame, which reduces the rate of free-radical reactions proceeding within the combustion zone [12, 13].

The effect of activated halloysite on the thermal decomposition rates of the vulcanizates investigated is very clear regardless of the structure of their spatial network. A considerable decrease in the thermal decomposition rate takes place especially in the case of the nanocomposites of nitrile rubber (Table 2).

A positive influence on the thermal decomposition rates of the vulcanizates of both nitrile rubbers (NSN8, and NSN15) and butadiene–styrene rubbers (SSN8, and SSN15), is exerted by the nucleus-sheath-type filler prepared for this study. Under the influence of this filler, not only the destruction rate of vulcanizates is decreased, but also the value of thermal decomposition residues is considerably increased,  $P_w$  (Table 2). The increased value of this parameter causes a decrease in the amount of destruction products passing to the flame, which reduces the yield of chemical reactions.

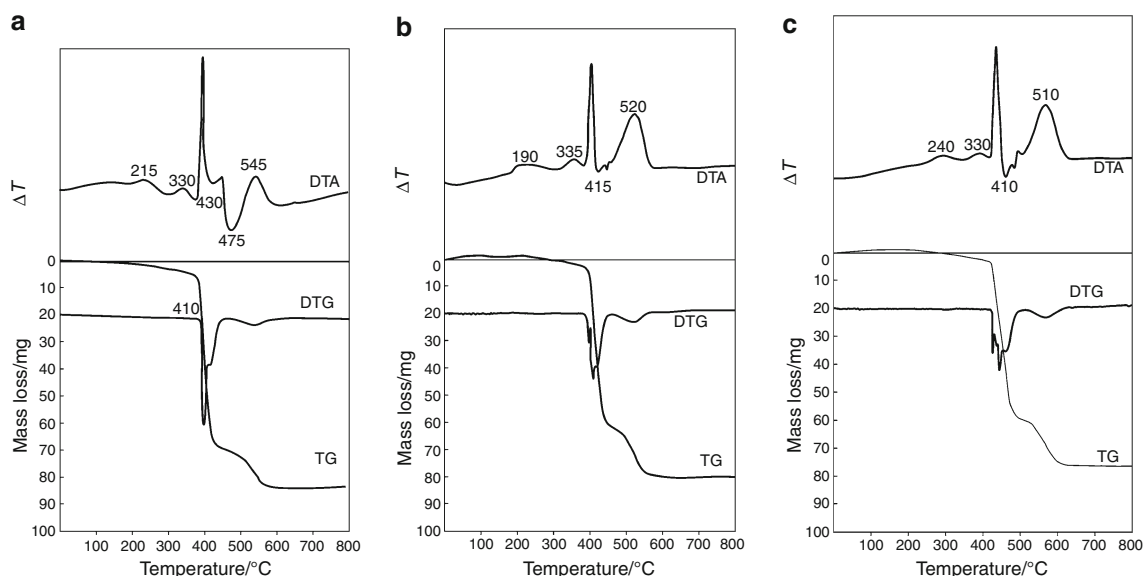


**Fig. 5** TG, DTG and DTA curves. **a** Peroxide vulcanizate of NBR rubber, NN. **b** Peroxide vulcanizate of NBR rubber containing 5 phr of activated halloysite, NNH5. **c** Sulfur vulcanizate of NBR rubber containing 5 phr of activated halloysite, NSH5

**Table 2** Thermal analysis of vulcanizates of NBR and SBR rubbers

Sample	$T_5/^\circ\text{C}$	$T_{50}/^\circ\text{C}$	$dm/dt/\text{mm}$	$T_R/^\circ\text{C}$	$T_{R\text{max}}/^\circ\text{C}$	$P_w/\%$	$T_s/^\circ\text{C}$	$P_{800}/\%$
NN	350	420	70	390	410	23	545	9
NNH5	390	420	57	370	410	24.5	510	11.1
NS	315	405	52	370	395	23	540	7
NSH5	370	415	46	380	400	27	530	10.0
NSH8	380	420	45	380	400	32	530	15.5
NSH15	360	415	45	370	400	31	530	16
NSN8	370	415	50	380	410	26.5	530	7.8
NSN15	370	415	50	370	410	32	530	11.1
SN	350	419	80	365	415	19	475	5
SNH5	360	410	76	370	400	20	480	7
SS	300	400	70	350	365	20	490	8.8
SSH5	320	400	70	350	370	20	480	8.9
SSH8	320	390	65	350	390	23	480	11.1
SSH15	360	400	75	360	400	21	470	10
SSN8	350	410	65	405	400	22	500	7.7
SSN15	330	400	65	460	400	23	480	8.8

$T_5$  and  $T_{50}$  are the temperatures of sample 5 and 50% mass loss, respectively,  $dm/dt$  is the maximum rate of thermal decompositions of vulcanizates,  $T_R$  is the initial temperature of thermal decompositions of vulcanizates,  $T_{R\text{max}}$  is the temperature of maximum rate of thermal decomposition of vulcanizate,  $P_w$  is the residue after the thermal decomposition of vulcanizate,  $T_s$  is the temperature of residue burning after the thermal decomposition of vulcanizate,  $P_{800}$  is the residue after heating up to  $T = 800^\circ\text{C}$ , *NN* is the peroxide vulcanizate of NBR rubber, *NNH5* is the vulcanizate *NN* containing 5 parts by wt. of halloysite per 100 parts by wt. of NBR, *NS* is the sulfur vulcanizate of NBR rubber, *NSHX* is the vulcanizate *NS* containing  $X$  parts by wt. of halloysite per 100 parts by wt. of NBR, where  $X = 5, 8, 15$ , *NSNX* is the vulcanizate *NS* containing  $X$  parts by wt. of nucleus-sheath type filler per 100 parts by wt. of NBR, where  $X = 5, 8, 15$ , *SN* is the peroxide vulcanizate of SBR rubber, *SNH5* is the vulcanizate *SN* containing 5 parts by wt. of halloysite per 100 parts by wt. of SBR, *SS* is the sulfur vulcanizate of SBR rubber, *SSHX* is the vulcanizate *SS* containing  $X$  parts by wt. of halloysite per 100 parts by wt. of SBR, where  $X = 5, 8, 15$ , *SSNX* is the vulcanizate *SS* containing  $X$  parts by wt. of nucleus-sheath type filler per 100 parts by wt. of SBR, where  $X = 5, 8, 15$

High  $P_w$  values are also observed in the case of the composites of nitrile rubber containing activated halloysite, while in the case of the vulcanizates of butadiene–styrene rubber, this parameter is practically unchanged. Therefore, it can be stated that halloysite facilitates the processes of thermal cyclization and nitrile rubber carbonization, which during its combustion is revealed by the formation of a thermally stable boundary layer impeding the flow of mass and energy between flame and sample. Halloysite fails to intensify carbonization processes taking place during the combustion of the composites of SBR rubber.

The results of derivatographic analysis also indicate a possibility of creating a boundary layer during the combustion of vulcanizates containing our filler (Table 2). Carbon particles present on the surface of aluminosilicate can facilitate the cyclization and thermal crosslinking of elastomer as well as fulfill the role of sorbents of volatile decomposition products.

The analysis of flammability test results leads us to conclude that both the activated halloysite and the filler obtained from it decrease the flammability of elastomers regardless of the structure of their spatial network (Table 3).

The increase in the halloysite content in elastomer nanocomposite is accompanied by the decrease in its flammability expressed by OI, combustion time in air ( $T_s$ ) as well as the maximal heat emission rate ( $\text{HRR}_{\text{max}}$ ). It should be noticed that the radical decrease in parameter  $\text{HRR}_{\text{max}}$  takes place in the case of samples containing the nucleus-sheath filler (vulcanizates denoted with symbols *SN8*, *NSN15*, *SSN8* and *SSN15*). In the case of the sulfur vulcanizate of SBR rubber containing the synthesized filler (*SSN15*), the maximal heat emission rate was reduced by more than 35% in relation to the unfilled sulfur vulcanizate of this polymer.

From the relevant literature data it follows that the reduction in polymer flammability results first of all from

- the formation of thermally stable isolating boundary layer,
- the reduction in the surface of contact between air and flammable gases resulting from polymer destruction,
- the modification of free-radical reactions taking place in the gaseous phase of combustion,
- decreased surface of the polymer-flame contact,



**Table 3** Flammability test results of vulcanizates of NBR and SBR rubbers

Sample	OI	Combustion time in air/s	$T_z/^\circ\text{C}$	$\text{HRR}_{\text{max}}/\text{W/g}$	Total HR/kJ/g	HR Capacity/J/g $\times$ K	Loss mass/%	Oxygen consumption/%
NN	0.205	276	357	472	34.0	479	11.47	50.02
NNH5	0.220	336	362	413	30.4	423	7.11	45.86
NS	0.215	289	366	432	32.0	432	9.46	67.09
NSH5	0.220	300	365	413	30.7	418	7.73	47.80
NSH8	0.225	336	369	396.1	29.8	399	9.01	29.33
NSH15	0.237	385	366	391.0	29.7	398	19.8	44.20
NSN8	0.245	370	363	345.4	31.3	412	4.13	29.52
NSN15	0.255	400	366	350	31.2	420	9.80	39.21
SN	0.210	194	350	450	34.5	501	21.11	40.11
SNH5	0.215	284	357	356.7	30.5	353	1.26	30.94
SS	0.220	273	355	399.8	34.3	397	14.31	44.91
SSH5	0.230	319	369	367.2	31.8	363	8.32	39.71
SSH8	0.236	325	365	380.1	32.3	382	21.33	52.08
SSH15	0.250	345	360	370.3	31.5	370	19.8	44.26
SSN8	0.257	341	374	359.1	35.5	358	9.04	40.27
SSN15	0.262	327	387	257.7	31.7	336	6.04	39.80

$T_z$  temperature of ignition,  $\text{HRR}_{\text{max}}$  maximum heat release rate

- the increased contents of non-flammable gaseous products such as water vapor or hydrohalide in the gaseous products of the polymer thermal decomposition [14, 15].

Both from the literature and our studies, it follows that the barrier properties of the halloysite nanotubes used in this study play a great role in reducing the flammability of nanocomposites. Aluminosilicate is impermeable for vapors and gases, and so during the thermal decomposition of nanocomposite, the low-molecular products due to thermal decomposition can diffuse outside elastomer only through closely defined spaces between nanotubes (the so-called channel effect) [16, 17].

The diffusion of oxygen into nanocomposite is also considerably impeded, as indicated by the value of percentage oxygen consumption (Table 3), which reduces the yield of radical degradation reactions and polymer depolymerization during its combustion, consequently increasing its resistance to the action of flame [18].

We believe that, apart from barrier effects, the lumen of the HNTs plays the leading role in decreasing the flammability of the nanocomposites. During the initial degradation stage of nanocomposites the degradation products of vulcanizates of diene rubbers may considerably be entrapped into the lumens of HNTs, resulting in higher randomness of lumen ends. The lumen could, therefore, entrap the degradation products more effectively [19].

From the results of elementary analysis, it follows that the filler obtained by us contains 7.53% by weight of

**Table 4** Mean values of the parameters of SBR rubber vulcanizates determined by means of cone calorimeter

Sample	SS	SSH8
Time to sustained ignition (TTI) [s]	55.01	51.86
Total heat release (THR) [ $\text{MJ} \times \text{m}^{-2}$ ]	73.37	71.97
Peak heat release rate ( $\text{HRR}_{\text{max}}$ ) [ $\text{kW} \times \text{m}^{-2}$ ]	1391.71	1094.59
Average heat release rate [ $\text{kW} \times \text{m}^{-2}$ ]	414.07	403.06
Average heat release rate (HOC) [ $\text{MJ} \times \text{m}^{-2}$ ]	35.33	34.29
Average mass lost rate (MLR) [ $\text{g} \times \text{s} \times \text{m}^{-2}$ ]	20.8	17.99
Average specific extinction area (SEA) [ $\text{m}^2 \times \text{kg}^{-1}$ ]	1122.26	1180.56
Average CO yield [ $\text{kg} \times \text{kg}^{-1}$ ]	0.0713	0.0769
Average CO <sub>2</sub> yield [ $\text{kg} \times \text{kg}^{-1}$ ]	2.2456	2.4157
Fire hazard ( $1/t_{\text{flasover}}$ ) [ $\text{kW} \times \text{m}^{-2} \times \text{s}^{-1}$ ]	25.29	21.10
Relative toxic fire hazard (RTFH <sub>CO/CO2</sub> )	0.0115	0.0113

chlorine [9]. In the early stage of the combustion of vulcanizate containing the filler in question, hydrogen chloride is emitted considerably, impeding the ignition of filled elastomeric materials as indicated by the values of ignition temperature ( $T_z$ ). The sulfur vulcanizate of SBR rubber containing that filler shows a higher ignition temperature

by about 30 °C in relation to the unfilled elastomer. The emitting hydrogen chloride also inhibits radical reactions taking place in flame, first of all, the oxidation of CO to CO<sub>2</sub>, which is the main source of heat during the combustion of polymers and polymeric materials (Table 3).

The results obtained by the cone calorimetry indicate that halloysite exerts an influence on the fire hazard posed by the elastomers containing this filler (Table 4). The smaller fire hazard of the nanocomposite of butadiene–styrene rubber (SSH8), in relation to the unfilled sulfur vulcanizate of this rubber (SS), results from the comparison of parameters, such as the average heat emission rate (HRR<sub>max</sub> and HRR), average specific combustion heat (HOC), and average mass loss rate (MLR). However, under the influence of the nanofiller, the average optical fume density is increased (SEA). This seems to result from the presence of carbon on the surface of aluminosilicate, facilitating the formation of carbon black, a main component of fume (Table 1).

## Conclusions

Regardless of the structure of the spatial network of elastomers, the activated halloysite considerably decreases the rate of their decomposition under thermo-oxidative conditions, and consequently reduces the flammability of the nanocomposites under investigation as confirmed by OI, combustion time in air and ignition temperature. The latter parameter increases especially in the case of the vulcanizates containing the nucleus-sheath-type filler.

The reduced flammability of the nanocomposites investigated results from the excellent barrier properties of the nanoadditives used as well as from emitting HCl in the case of the nucleus-sheath type filler.

The use of the modified halloysite as filler of diene elastomers also allows the reduction in their fire hazard.

**Open Access** This article is distributed under the terms of the Creative Commons Attribution Noncommercial License which permits any noncommercial use, distribution, and reproduction in any medium, provided the original author(s) and source are credited.

## References

1. Achilias DS, Nikolaidis AK, Karayannidis GP. PMMA/organo-modified montmorillonite nanocomposites prepared by in situ bulk polymerization. *J Therm Anal Calorim.* 2010;102:451–60.

2. Lalikova S, Pajtasova M, Ondrusova D, Bazylakova T, Olsovsky M, Jona E, Mojumdar SC. Thermal and spectral properties of natural bentonites and their applications as reinforced nanofillers in polymeric materials. *J Therm Anal Calorim.* 2010;100:745–9.
3. Gilman W. Flammability and thermal stability studies of polymer layered-silicate (clay) nanocomposites. *Appl Clay Sci.* 1999;15: 31–49.
4. Handge UA, Hedicke-Hochstotter K, Altstadt V. Composites of polyamide 6 and silicate nanotubes of mineral halloysite: influence of molecular weight on thermal and rheological properties. *Polymer.* 2010;51:2690–9.
5. Guo B, Chen F, Lei Y, Liu X, Wan J, Jia D. Styrene–butadiene rubber/halloysite nanotubes nanocomposites modified by sorbic acid. *Appl Surf Sci.* 2009;255:7329–36.
6. Roj S, Das A, Thakur V, Mahaling RN, Bhowmick AK, Heinrich G. Preparation and properties of natural nanocomposites based on natural rubber and naturally occurring halloysite nanotubes. *Mater Des.* 2010;31:2151–6.
7. Levis SR, Deasy PB. Characterisation of halloysite for use a microtubular drug delivery system. *Int J Pharm.* 2002;243:125–34.
8. Joussein E, Petit S, Delvaux B. Behavior of halloysite clay under formamide treatment. *Appl Clay Sci.* 2007;35:17–24.
9. Janowska G, Rzymiski W, Kmiołek M, Kucharska A, Kasiczak A. Właściwości termiczne i palność chlorosulfonowanego polietyleny. *Polimery.* 2009;4:243–324.
10. Zhao M, Liu P. Halloysite nanotubes/polystyrene (HNTs/PS) nanocomposites via in situ bulk polymerization. *J Therm Anal Calorim.* 2008;94:103–7.
11. Rybiński P, Janowska G. Influence of network structures of nitrile rubbers on their thermal properties. *Polimery.* 2009;54:275–82.
12. Janowska G, Rybiński P, Jantas R. Effect of the modification of silica on thermal properties and flammability of cross-linked butadiene–acrylonitrile rubbers. *J Therm Anal Calorim.* 2007;87: 511–7.
13. Rybiński P, Janowska G, Ślusarski L. Influence of cryogenic modification of silica on thermal properties and flammability of cross-linked nitrile rubber. *J Therm Anal Calorim.* 2010;101: 665–70.
14. Janowska G, Przygocki W, Włochowicz A. Palność polimerów i materiałów polimerowych WNT, Warszawa 2007, ISSN: 978-83-204-3299-2, 340 stron.
15. Rybiński P, Janowska G. Effect of flame retardants on thermal stability and flammability of cured nitrile rubber. *Polimery.* 2009;11–12:833–9.
16. Leszczyńska A, Njuguna J, Pielichowski K, Benerjee JR. Polymer/montmorillonite nanocomposites with improved thermal properties. Part I. *Thermochim Acta.* 2007;453:75–96.
17. Janowska G, Kucharska-Jastrzębek A, Rybiński P. Thermal stability, flammability and fire hazard of butadiene-acrylonitrile rubber nanocomposites. *J Therm Anal Calorim.* doi:10.1007/s 10973-010-1282-y
18. Marney DCO, Russell LJ, Wu DY, Nguyen T, Cramm D, Rigopoulos N, Wright N, Greaves M. The suitability of halloysite nanotubes as fire retardant for nylon 6. *Polym Degrad Stab.* 2008;93:1971–8.
19. Mingliang Du, Baochun Guo, Demin Jia. Thermal Stability and flame retardant effects of halloysite nanotubes on poly(propylene). *Eur Polym J.* 2006;42:1362–9.